Available online at www.sciencedirect.com

SCIENCE DIRECT®

Lithos 83 (2005) 277–298

LITHOS

www.elsevier.com/locate/lithos

Relationship between the Layered Series and the overlying evolved rocks in the Bjerkreim-Sokndal Intrusion, southern Norway

J. Richard Wilson[a,*], Gitte Overgaard[b]

[a]*Department of Earth Sciences, Aarhus Universitet, 8000 Århus C, Denmark*
[b]*Kærvej 6, Danstrup, 8860 Ulstrup, Denmark*

Received 25 August 2003; accepted 18 February 2005
Available online 18 April 2005

Abstract

The Bjerkreim-Sokndal layered intrusion (BKSK) consists of a >7000-m-thick Layered Series comprising anorthosites, leuconorites, troctolites, norites, gabbronorites and jotunites (hypersthene monzodiorites), overlain by an unknown thickness of massive, evolved rocks: mangerites (hypersthene monzonites; MG), quartz mangerites (QMG) and charnockites (CH). The Layered Series is subdivided into six megacyclic units that represent the crystallisation products of successive major influxes of magma. We have studied a ca. 2000-m-thick section that straddles the sequence from the uppermost part of the Layered Series to the QMG in the northern part of the intrusion. Mineral compositions in 37 samples change continuously in the lower part of the sequence up to the middle of the MG-unit (plagioclase An37-18; olivine Fo40-7; Ca-poor pyroxene Mg#57-15; Ca-rich pyroxene Mg#65-21). Above this compositions are essentially constant in the upper part of the MG-unit and in the QMG (An21-13; Fo6-4; Mg#opx17-13; Mg#cpx25-20). The amount of interstitial quartz and the amount of normative orthoclase, however, both increase systematically upwards through the QMG-unit, implying that these rocks are cumulates. There is no evidence of a compositional break in the MG-QMG sequence that could reflect influx of relatively primitive magma.

Two types of QMG/CH are known in the uppermost part of BKSK. Olivine-bearing types are comagmatic with the underlying Layered Series; the studied stratigraphic sequence belongs to this suite. Two-pyroxene QMG and amphibole CH define a separate compositional lineage related to jotunites. An intrusive unit of dominantly two-pyroxene QMG is discordant to the olivine-bearing jotunite-MG-QMG sequence near Rapstad, confirming the presence of two compositionally distinct suites of QMG and related lithologies in the upper part of BKSK.

A xenolith-rich unit near the olivine-bearing MG-QMG boundary represents a major collapse of the roof of the magma chamber during the final stages of crystallisation.
© 2005 Elsevier B.V. All rights reserved.

Keywords: Bjerkreim-Sokndal Intrusion; Layered intrusion; Gabbronorite; Jotunite; Mangerite; Charnockite

* Corresponding author. Tel.: +45 8942 2526; fax: +45 8942 2525.
E-mail address: jrw@geo.au.dk (J.R. Wilson).

0024-4937/$ - see front matter © 2005 Elsevier B.V. All rights reserved.
doi:10.1016/j.lithos.2005.03.006

1. Introduction

The Bjerkreim-Sokndal Intrusion (BKSK) (Michot, 1960, 1965; Duchesne, 1987; Wilson et al., 1996) occupies an area of about 230 km^2 in southern Norway (Fig. 1), and is a post-orogenic pluton belonging to the Late Proterozoic Rogaland Anorthosite Province. The intrusion comprises lithologies of the anorthosite kindred: anorthosite, troctolite, leuconorite, norite, gabbronorite, jotunite (monzonorite), mangerite (MG)(hypersthene monzonite), quartz mangerite (QMG) and charnockite. In this respect it is petrologically important since it links anorthosites and charnockites, with all intermediate lithologies, in a single intrusion. The lower part of the BKSK, the Layered Series, consists dominantly of modally layered cumulates sub-divided into six megacyclic units. The Layered Series is overlain by dominantly massive,

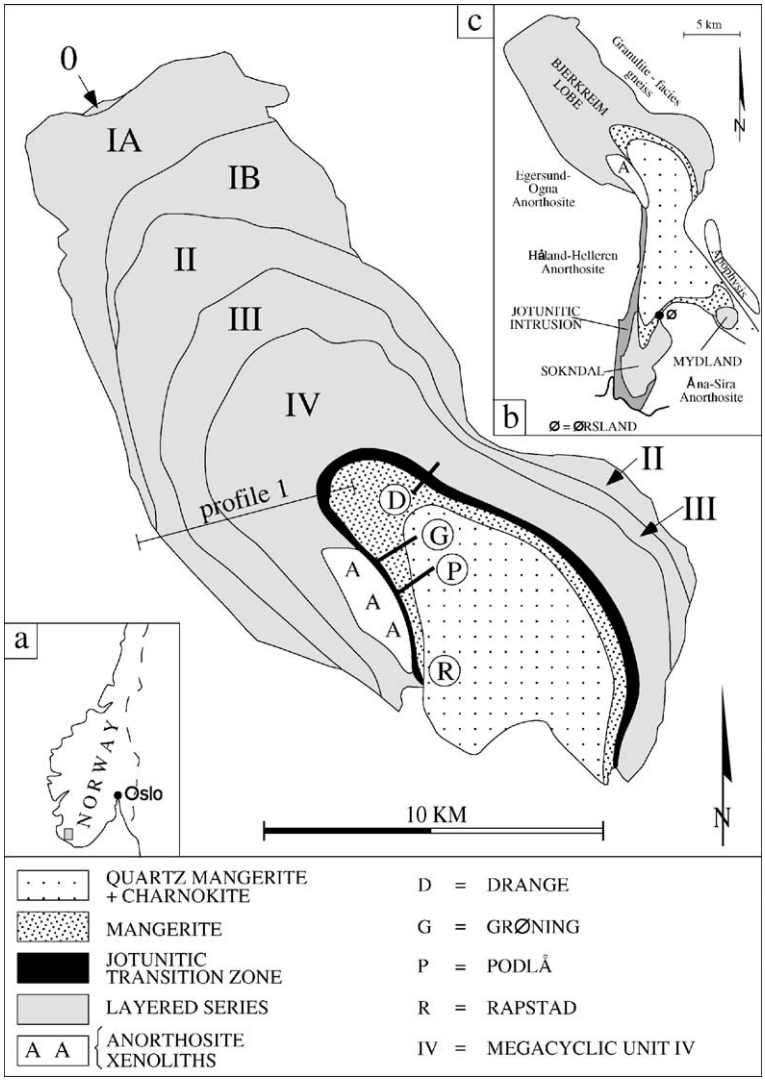

Fig. 1. (a) Location of (b) in southern Norway. (b) Simplified geological map of the Bjerkreim-Sokndal layered intrusion identifying the Bjerkreim, Sokndal and Mydland lobes. (c) Bjerkreim lobe of the Bjerkreim-Sokndal intrusion showing the distribution of megacyclic units 0–IV and the location of sub-profiles at Drange (D), Grøning (G) and Podlå (P). The location of the Rapstad area (R) is also indicated. Based largely on Fig. 1 in Wilson et al. (1996). Cumulate stratigraphic variations along profile 1 are shown in Fig. 2.

evolved lithologies that comprise MG, QMG and charnockite. Paul Michot, who carried out pioneering work in the BKSK and surrounding rocks, favoured a comagmatic origin for the Layered Series and the overlying, massive rocks (Michot, 1960, 1965). The relationship between the Layered Series and the overlying rocks has subsequently been controversial (Michot and Pasteels, 1969; Pasteels et al., 1970; Duchesne and Demaiffe, 1978; Demaiffe et al., 1979; Wielens et al., 1980; Wiebe, 1984; Duchesne et al., 1987; Nielsen et al., 1996; Wilson et al., 1996; Duchesne and Wilmart, 1997). Here we present new mineral and whole-rock data from sample profiles across the boundary between the Layered Series and the overlying rocks in the northwestern part of BKSK (the Bjerkreim lobe). Our data support the recent suggestion of Duchesne and Wilmart (1997) that at least some of the evolved rocks are cogenetic with the underlying Layered Series. This work is largely based on the unpublished MSc thesis of the second author (Overgaard, 1998) that was carried out under supervision of the first author.

2. The Bjerkreim-Sokndal layered intrusion

The BKSK intrudes granulite facies gneisses and massif-type anorthosites, including the Egersund-Ogna and Åna-Sira bodies, and locally contains numerous xenoliths of these lithologies. BKSK and the massif-type anorthosites were emplaced in a short time interval at 931 ± 2 Ma (Schärer et al., 1996). The intrusion, which extends for ca. 40 km from northwest to southeast, consists of a main lobe (Bjerkreim) and two minor ones (Sokndal and Mydland) (Fig. 1). Monzonoritic dykes and minor intrusions are locally numerous in BKSK; these are not shown in Fig. 1. The arrangement of lithological units in the Bjerkreim lobe defines a syncline that plunges southeast at 20–40°. The axial trace is curved and plunges ca. 40° north in the Sokndal lobe so that the massive, evolved rocks (MG, QMG and charnockites) are located in the core of a doubly-plunging syncline.

Based on repeated modal variations with stratigraphic height, Paul Michot (1960, 1965) divided the Bjerkreim lobe into five rhythmic units that reflect the crystallisation products of repeated magma influxes (Duchesne, 1972). The rhythmic units have been revised (Wilson et al., 1996) but Michot's numbering system has been retained as far as possible in that his original units 2, 3 and 4 are referred to as II, III and IV, in agreement with papers by Nielsen and Wilson (1991) and Jensen et al. (1993). The existence of P. Michot's unit 5 has not been confirmed (Nielsen and Wilson, 1991; Wilson et al., 1996) and unit IV grades upwards into a jotunitic Transition Zone (TZ) that directly underlies the more evolved rocks (Fig. 2). Since the sequence of lithologies in the individual "rhythmic units" is believed to reflect the fractional crystallisation of repeated influxes of magma the term megacyclic unit (MCU) is preferred, in keeping with the recommended terminology for layered intrusions of Irvine (1982).

Each MCU comprises a characteristic sequence of cumulates. Here we concentrate on the uppermost megacyclic unit, MCU IV, and the overlying lithologies. Crystallisation of each of the lower MCUs was interrupted by the influx of new magma and MCU IV therefore shows the most complete sequence of cumulates. There is a marked compositional regression at the base of MCU IV where the uppermost rocks belonging to MCU III (zone IIIe; plagioclase–Ca-poor pyroxene–Ca-rich pyroxene–ilmenite–magnetite–apatite cumulates) are overlain by plagioclase (± ilmenite ± Ca-poor pyroxene) cumulates (zone IVa). These are in turn overlain by troctolitic cumulates (IVb) which are amongst the most primitive lithologies in BKSK. These olivine-bearing cumulates are succeeded by ilmenite norites (IVc), magnetite norites (IVd) and apatite-bearing gabbronorites (IVe) with the successive entry of cumulus magnetite before the simultaneous appearance of Ca-rich pyroxene and apatite. The Ca-poor pyroxene is inverted pigeonite and plagioclase is commonly antiperthitic in zone IVf. This is followed by the entry of cumulus iron-rich olivine that defines the base of the TZ; this more or less coincides with the occurrence of interstitial perthitic feldspar (Duchesne et al., 1987). The appearance of cumulus mesoperthite defines the base of the MG unit. The presence of >5% modal quartz defines the base of the QMG unit. Zircon is a common accessory phase in the QMG. Duchesne and Wilmart (1997) recognised that the QMGs are intermingled with quartz-rich varieties that should be classified as charnockites.

Modal layering is a major feature of most of the Layered Series, including the TZ. Cumulate textures are, however, commonly obscured as a result of locally

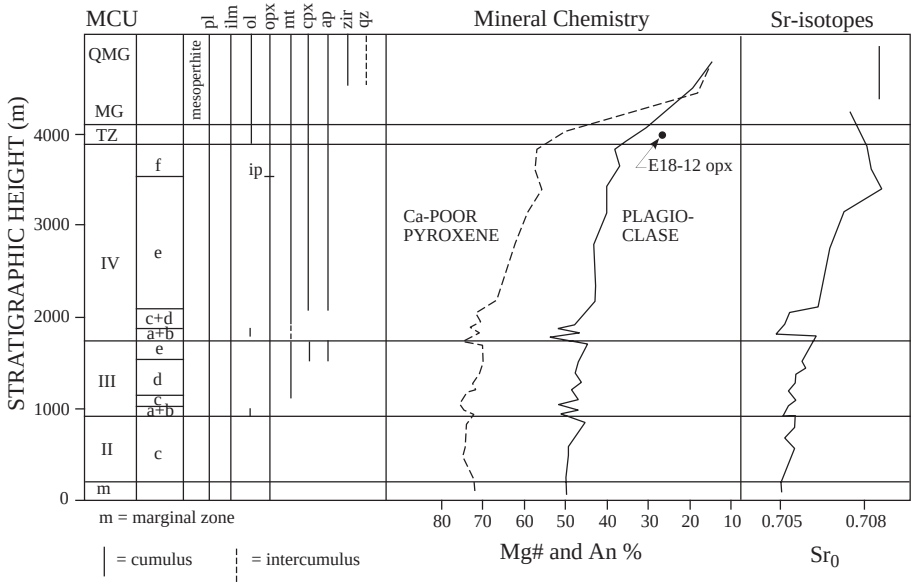

Fig. 2. Generalised stratigraphy of the Bjerkreim-Sokndal Layered Series and compositional variation with stratigraphic height of Ca-poor pyroxene, plagioclase and whole-rock Sr-isotopic ratios. Based on Fig. 5 in Wilson et al. (1996) except mineral compositions for the TZ (jotunitic Transition Zone), MG (mangerite) and QMG (quartz mangerite) where averages for these units are from the present work (TZ Mg#opx:An% 50:30; MG 21:20; QMG 15:15). The sequence shown is developed along profile 1 in Fig. 1. The Mg# content of Ca-poor pyroxene in TZ sample E18-12 (from Fig. 2 and Table 1 in Nielsen et al., 1996) is also shown. This sample has a Sr_0 ratio of 0.71094. These compositions are very different from those of our TZ samples and we question whether sample E18-12 is truly representative of the TZ. See text for details.

extensive recrystallisation of plagioclase to polygonal aggregates. Cumulates are commonly foliated, generally in the plane of the modal layering, and cumulus minerals may form augen in a foliated matrix. Linear fabrics are locally developed, especially around the hinge of the syncline. The foliation, lineation and synclinal form of the Layered Series developed by the inverse diapirism of BKSK under granulite facies conditions as a result of its situation within lower density gneisses and anorthosite massifs (Paludan et al., 1994; Glazner, 1994). The lowest part of the MG unit is locally characterised by modal layering but the upper part and the overlying QMG and charnockites in the core of the syncline are generally massive. Mineral lamination defined by the parallel orientation of feldspar crystals is locally developed.

A locally important feature of BKSK is the presence of country rock inclusions. Anorthositic inclusions dominate in the lower part of the Layered Series and are believed to represent fragments of adjacent anorthosite massifs. This is evidence that emplacement of BKSK post-dated at least some of the Rogaland anorthosites. Michot (1961) interpreted a tongue-shaped body of anorthositic rocks in the southern part of the Bjerkreim lobe as belonging to the Haaland-Helleren massif that intruded BKSK layered rocks (Fig. 1c). However, Nielsen et al. (1996) and Wilson et al. (1996) re-interpreted this anorthositic "tongue" as a partially dismembered large inclusion. BKSK is consequently younger than all the Rogaland massif-type anorthosites. Xenoliths of quartzo-feldspathic gneiss and mafic granulite are locally abundant in the upper part of the Layered Series, and large blocks are fairly common in the upper part of MCU IV and the TZ.

The interval near the margin between the MG and QMG is locally characterised by abundant xenoliths and was referred to as the "septum xenolithique" by Michot (1960). In the Ørsland area (Fig. 1b), Duchesne et al. (1987) and Duchesne and Wilmart (1997) describe the contact between the MG and QMG as crowded by inclusions of quartzo-feldspathic to noritic gneisses of various grain sizes. A noteworthy feature of this interval is the presence of cm- to m-sized, fine-grained, rounded jotunitic inclusions. Wiebe (1984) referred to these bodies as pillows and

considered that they were evidence of the mingling of two magmas, one parental to the MG/QMG belonging to BKSK and the other an intruded jotunite.

Duchesne and Wilmart (1997) identified two types of QMG and charnockite, principally on the basis of the nature of the mafic phases present. One type contains olivine and clinopyroxene, whereas the other contains two pyroxenes and no olivine. Some two-pyroxene charnockites also contain poikilitic calcic amphibole and are referred to as amphibole charnockites. As will be discussed later, Duchesne and Wilmart (1997) considered that the olivine-bearing lithologies are genetically related the BKSK Layered Series whereas the two-pyroxene and amphibole-bearing varieties represent a separate intrusion.

Michot (1960) and Duchesne (1972) considered that the Layered Series and the overlying, evolved rocks were related by a continuous differentiation process. Based on observations in the Mydland area, Rietmeijer (1979) interpreted the massive, evolved rocks located in the core of the syncline as being discordant to and younger than the Layered Series.

Demaiffe et al. (1979, 1986) found that the $^{87}Sr/^{86}Sr$ isotopic compositions of the MG and QMG (0.7085) and of plagioclase cumulates belonging to the Layered Series (0.705–0.706) precluded that they could be related to each other by fractional crystallisation. Nielsen et al. (1996) showed, however, that there was a gradual increase in Sr-isotopic ratios through the upper part of the Layered Series (0.7049 at the base of MCU IV) to the overlying, evolved rocks (0.7085), and concluded that they were cogenetic (Fig. 2). The high Sr-isotopic ratios and some other geochemical features of the MG and QMG have generally been explained by assimilation of country rock gneisses in the roof zone of the intrusion that took place concurrently with fractional crystallisation (Demaiffe et al., 1979, 1986; Nielsen et al., 1996; Wilson et al., 1996; Duchesne and Wilmart, 1997).

Studies across the boundary between the Layered Series and the overlying evolved rocks have hitherto been restricted to the Ørsland area in the Sokndal lobe (Duchesne et al., 1987; Duchesne and Wilmart, 1997) where country rock inclusions and jotunitic pillows are relatively numerous (Fig. 1b). Here we study the boundary in the Bjerkreim lobe where the Layered Series has been thoroughly described. We present whole-rock geochemical and mineral chemical data of samples across the boundary together with graphical presentation of extensive additional mineral chemical data from the Layered Series.

Recent mapping (Brian Robins, 2002, personal comunication) has revealed that massive, broadly quartz mangeritic rocks in the Rapstad area are discordant to the Layered Series and cut across the MCU IVf-TZ-MG sequence (Fig. 1). It is plausible that this discordant unit represents a "separate intrusion of two-pyroxene quartz mangerite" identified on the basis of mineralogical and chemical criteria by Duchesne and Wilmart (1997). It could also explain the discordant nature of the evolved rocks to the Layered Series in the Mydland area reported by Rietmeijer (1979). This topic will be briefly explored later.

3. Boundary between the Layered Series and the overlying evolved rocks

3.1. Sample profiles

Exposures, accessibility and the abundance of xenoliths along the SW limb of the Bjerkreim syncline do not allow continuous sampling of a single profile that would cover the entire interval from the upper part of MCU IV through the QMG in the Bjerkreim lobe of BKSK. A profile (Fig. 4) has therefore been compiled from three sub-profiles (Fig. 1c). Sub-profile D (Fig. 3a) was collected in the Drange area on the northern flank of the syncline and covers the interval from the upper part of MCU IV (6 samples), through the TZ (4) and into the basal part of the MG (3). Sub-profiles G and P were collected in the Grøning and Podlå areas respectively on the southern flank of the syncline. Along the northern flank this interval is inaccessible because of steep slopes and vegetation. The southern flank is more suitable for study but field relations are complicated here by the presence of abundant anorthositic enclaves mentioned earlier (Fig. 1c). Sub-profile G (Fig. 3b) includes the MG (10) and extends into the QMG (2). The boundary between the MG and QMG in the field has been drawn where macroscopic quartz is consistently present; this coincides with about 5% modal quartz. The lowermost sample in the Grøning sub-profile (G30; Fig. 3b) is from an anorthositic xenolith.

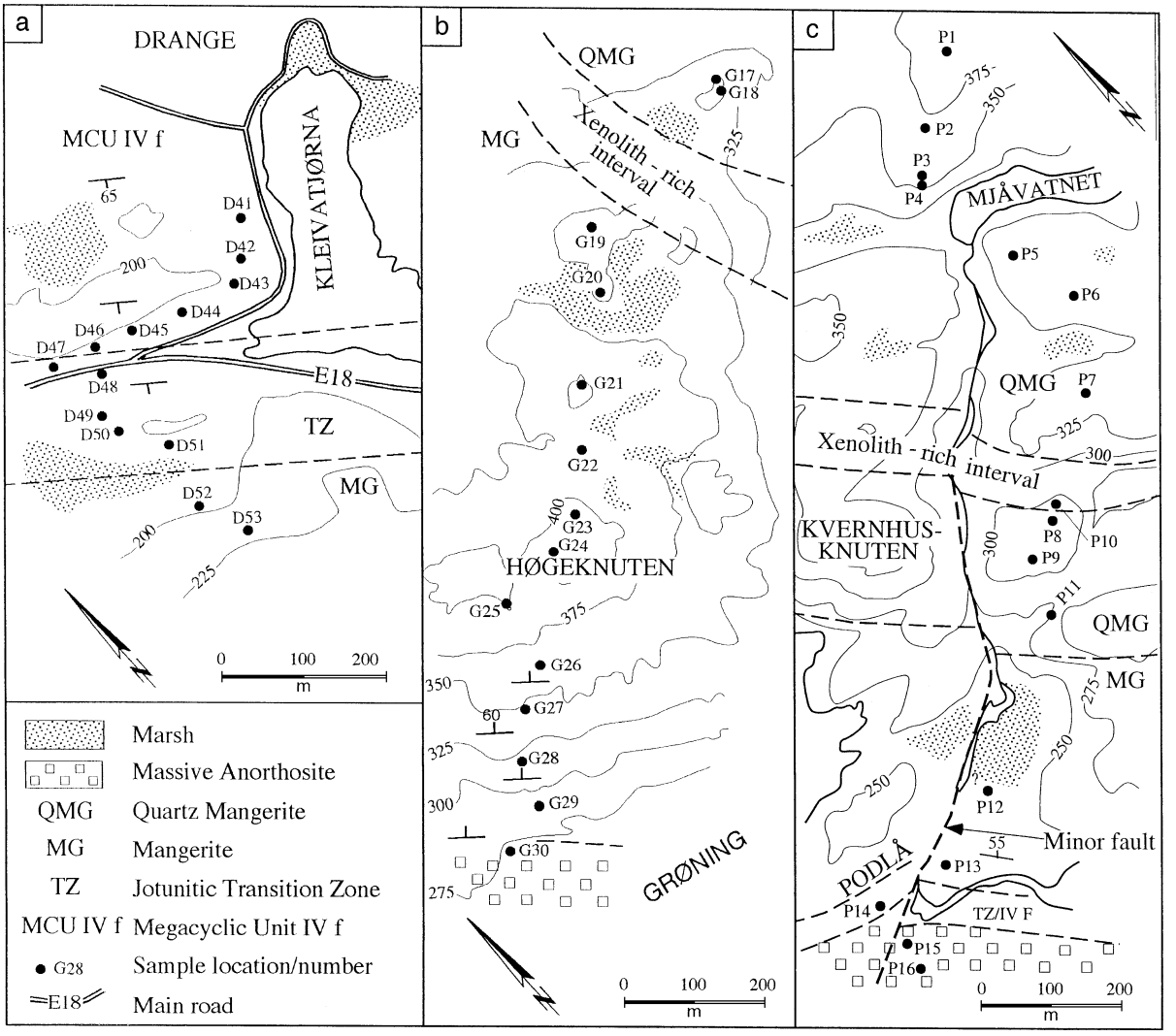

Fig. 3. Sample localities and field relations in the (a) Drange, (b) Grøning and (c) Podlå sub-profiles.

The TZ is not exposed in the Grøning sub-profile. The Podlå sub-profile largely represents a section through the QMG-unit (11). The lowest macroscopic occurrence of quartz is just below sample P11. It will be shown later that samples P13 and P14 (from the TZ) have compositions inconsistent with their apparent stratigraphic locations. No weight will be placed on samples P13 and P14 in interpretations below and they have been omitted from Fig. 4. The lowermost Podlå samples (P15, P16) are from an anorthositic inclusion. The boundary between the TZ and the MG is used as the reference datum (=0 m level) in Fig. 4.

A xenolith-rich interval (ca. 100 m-thick) coincides with the MG-QMG boundary in the Grøning sub-profile, whereas in the Podlå sub-profile the interval (ca. 80-m thick) is present some 200 m above this boundary, entirely within the QMG (Fig. 3). The location of the xenolith-rich interval in Fig. 4 is based on the Podlå profile. This gives rise to a problem with regard to the placing of samples G17 and G18 in Fig. 4. They are above the xenolith-rich interval in Fig. 3 and definitely less than 270 m above sample G19 (assuming that the QMG is vertical here). In Fig. 4 these samples have been located at their estimated

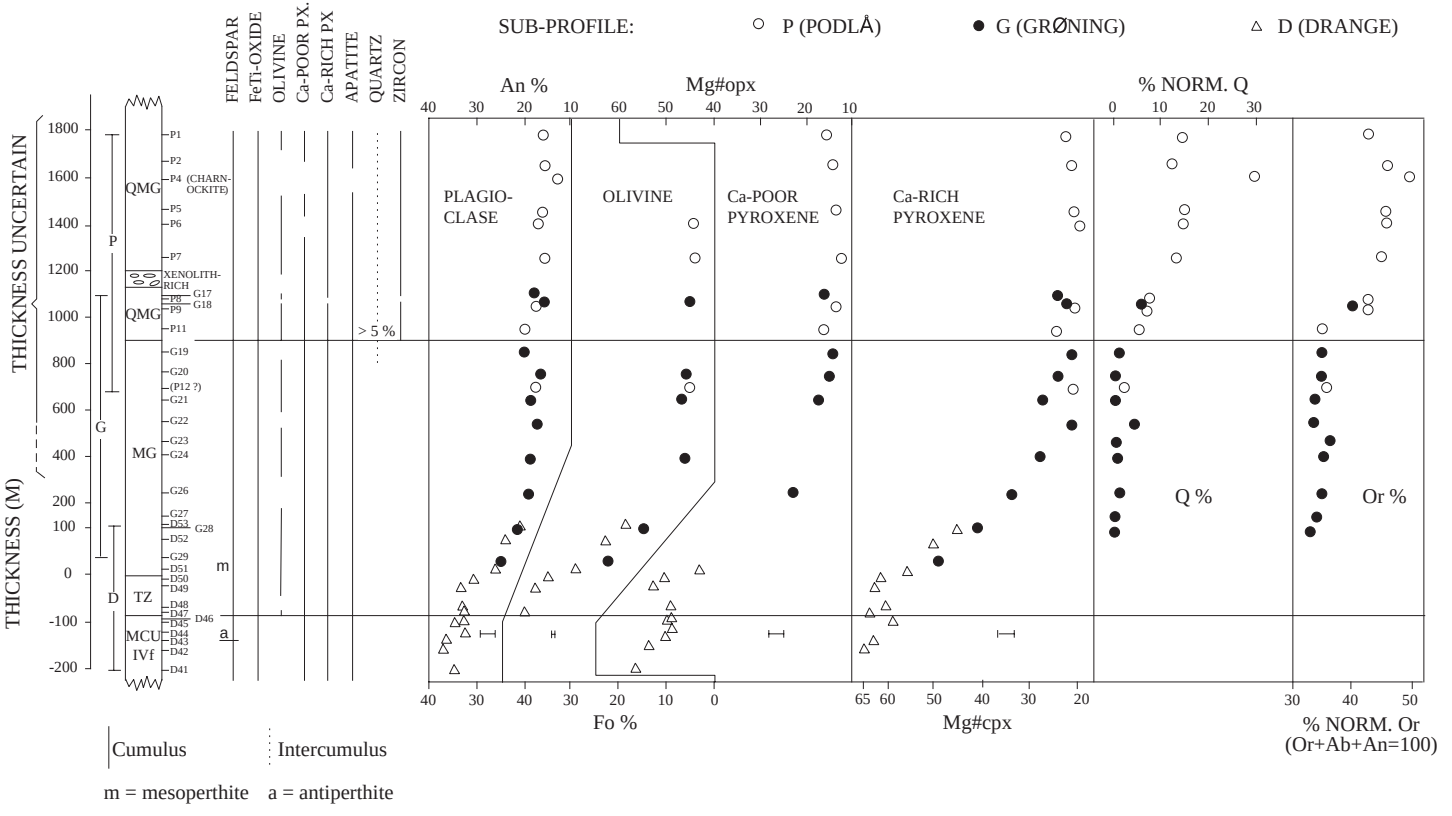

Fig. 4. Compiled profile from the upper part of the Layered Series to the quartz mangerites in the Bjerkreim lobe of the Bjerkreim-Sokndal layered intrusion. From left to right: stratigraphic thickness (uncertain above ca. 400 m, note the change of scale between 100 m and 200 m); identification of sub-profiles from which the figure is compiled (D=Drange; G=Grøning; P=Podlå); zonal subdivision; stratigraphic locations of samples; cumulate stratigraphy; variation of An% in plagioclase, Fo% in olivine, Mg# (=100 Mg/(Mg+Fetot)) in Ca-poor and Ca-rich pyroxenes; CIPW-normative quartz; CIPW-normative orthoclase (calculated as Or+Ab+An=100). Error bars in the lower parts of the plots are at the two standard deviation level. Plagioclase analyses up to the TZ-MG boundary represent cumulus grains. In the MG and QMG they are of granular plagioclases that have probably exsolved from mesoperthite.

stratigraphic height above sample G19. Xenoliths were avoided during sample collection. The thickness of sub-profile D (310 m) has been estimated on the basis of a consistent southerly dip of 65° (strike=113°) for modal layering in MCU IV and in the TZ in the Drange area. Thicknesses in sub-profile G are more difficult to estimate since only the lowermost rocks (up to G26) contain modal layering (dip=60–70°NE). Some of the MGs and QMGs in this area, however, have a steep foliation (strike N150°E, dip 70–90°NE), consistent with the orientation of the magnetic foliation in this area (Bolle et al., 2000). We have therefore used a dip of 65°NE for the lower part of sub-profile G, increasing to 80°ENE at the top. Sub-profile P consists entirely of massive, unlayered rocks and we have adopted an average dip of 80°NE, consistent with the orientation of the field and magnetic foliations. It is apparent from Fig. 9 in Bolle et al. (2000) that the top of sub-profile P is close to the axial zone of the syncline. It therefore emerges that the TZ is about 90 m thick in sub-profile D, well within the range of 50–200 m quoted by Duchesne and Wilmart (1997). The MG-unit is about 900 m thick in sub-profile G and a thickness of about 900 m of QMG (and charnockite) has been sampled in sub-profile P.

It is apparent that the thickness of the MG-unit decreases significantly from Grøning southwards towards Podlå. At Grøning, where the MG/QMG boundary coincides with the xenolith-rich interval, it is about 900 m thick. At Podlå, on the other hand, there is a thickness of ca. 300 m from the top of the TZ to the level at which there is >5% macroscopic quartz, and a further 180 m to the xenolith-rich interval.

Within the individual sub-profiles the stratigraphic sequence of samples is not in doubt (apart from at the base of sub-profile P, as mentioned above), but the exact relative placing of samples from different sub-profiles in Fig. 4 is inevitably rather subjective. This is relevant for the relationships of samples G17-18 in the QMG (mentioned above), P11-12 near the QMG-MG boundary and G28-29 and D52-53 near the base of the MG-unit. This aspect will be considered below.

3.2. Mineralogy and petrography

The rocks collected in this study from the top of MCU IV consist of cumulus plagioclase, FeTi-oxide, Ca-poor pyroxene, Ca-rich pyroxene and apatite (Fig. 4). The Ca-poor pyroxene is associated with abundant exsolved Ca-rich pyroxene and is interpreted as representing inverted pigeonite. This mineral assemblage is consistent with these rocks being assigned to cumulate zone IVf of Wilson et al. (1996). In the uppermost 50 m plagioclase becomes antiperthitic and alkali feldspar occurs as discrete interstitial grains.

The base of the TZ is defined by the first appearance of iron-rich olivine as an additional phase at −90 m. Olivine is present in all but one (D48) of the four jotunitic TZ samples. The base of the overlying MG-unit is defined by the appearance of abundant mesoperthitic alkali feldspar. Olivine is present in 11 of the 14 MG-samples. The appearance of >5% modal quartz defines the base of the QMG-unit. This coincides with the first appearance of zircon in the Podlå sub-profile. Fresh olivine is present in 3 of the 11 QMG-samples and 3 others contain heavily oxidised relicts. Ca-poor pyroxene is absent in one (P6), apatite is absent in one (P4) and both Ca-rich pyroxene and zircon are absent in one (P8). In addition to the phases shown in Fig. 4 there are small quantities of biotite and hornblende in all samples. The QMG (and MG) contains abundant mesoperthite together with small, minor plagioclase grains. The latter may represent plagioclase that has been released from mesoperthite during recrystallisation. Minor additional phases (apatite, zircon and Fe-Ti oxides) locally occur as inclusions in the main mafic minerals but also occur as discrete grains. Sample P4 contains ca. 30% quartz and is a charnockite.

It is clear in Fig. 4 that the amount of CIPW-normative quartz (Q) increases systematically with stratigraphic height from the uppermost MG samples through the QMG-unit, reaching ca. 15% Q in P5. Above this there is an abrupt increase to ca. 39% Q in P4 (charnockite) followed by 12–14.3% Q in the uppermost two samples (P1 and P2). This is accompanied by a small upward increase in normative orthoclase (Or) (expressed in terms of Or+Ab+An=100%) in the lower part of the MG (32.7% Or in G28 to 36.3% Or in G23) followed by fairly constant values (34.6±1.2% Or) up to the base of QMG. This is followed by an abrupt increase to values >40.4% Or in the QMG. Or reaches 49.7% in the charnockite before decreasing to 43–46% in P1 and P2.

Four samples (R1–4) from the Rapstad area (Fig. 1) that represent the discordant evolved unit are quartz mangerites (R2–4) and a quartz-bearing jotunite (R1). For the sake of convenience they will jointly be referred to as the Rapstad quartz mangerites. Strongly perthitic K-feldspar dominates over discrete plagioclase grains and quartz is a minor phase in R1 and reaches ca. 5–10 modal % in R2–4. Ca-poor pyroxene (inverted pigeonite) forms optically continuous oikocrysts whereas clinopyroxene occurs as anhedral grains together with minor hornblende, apatite, FeTi-oxides and zircon. Olivine is absent. The mineralogy and texture of these rocks is consistent with the two-pyroxene QMG lineage of Duchesne and Wilmart (1997).

3.3. Mineral chemistry

Mineral compositions have been determined by microprobe analyses at the Department of Earth Sciences, University of Aarhus, using a JEOL-JXA Superprobe equipped with one energy (EDS) and four wavelength dispersive (WDS) spectrometers. An acceleration voltage of 15 kV and a beam current of 15 nA were used throughout. Counting times for WDS were 40 s and for EDS 120 s for feldspars and 200 s for mafic minerals. Ti, Mn, Na, Cr and Ni were analysed using WDS and Si, Al, Fe, Mg and Ca by EDS in mafic minerals. In feldspars Fe, Na and K were analysed by WDS and Si, Al and Ca by EDS. Pyroxenes and olivine were analysed using a focused beam (ca. 2 μm diameter). Most of the feldspar analyses were carried out using a defocused beam with a diameter of ca. 5 μm. Most of the analyses plotted in Figs. 4–5 and listed in Tables 1 and 2 are averages of three points in each of three grains. Alkali feldspars are generally mesoperthitic with roughly equal quantities of K-rich and Na-rich phases. These have been analysed using a defocused beam (ca. 5 μm diameter) to avoid the loss of alkalies, and avoiding exsolution lamella as far as possible in order to determine the compositions of the Or- and Ab-rich parts of the mesoperthite. Between 20 and 40 points were analysed in each of three grains.

Standard deviations (s.d.), determined by repeated analysis of plagioclase ($An_{17.2}$), olivine ($Fo_{6.0}$) and Ca-rich pyroxene ($Mg\#cpx_{24.0}$) in a selected sample (G20) are as follows: plagioclase=1.04% An, olivine=0.28% Fo and Ca-rich pyroxene=1.28% Mg#cpx. Ca-poor pyroxene is assumed to have the same s.d. as Ca-rich pyroxene. These values are in general agreement with those used by, for example, Nielsen and Wilson (1991). Two s.d. values are shown in Figs. 4 and 5. Plagioclase, olivine and pyroxene compositions in eight representative samples are presented in Table 1. Compositions in all samples are available from the first author on request. Table 2 presents plagioclase An%, olivine Fo%, Mg# in pyroxenes and Or%/An% in mesoperthite for samples that have not been chemically analysed, whereas Table 3 presents this data together with whole rock chemistry.

Cumulus plagioclase, which is restricted to MCU IVf and the TZ in Fig. 4, covers a compositional range from $An_{37\text{-}30}$. In the lower part of the MG, granular plagioclases become gradually more sodic upwards (from An_{26} in D51 to $An_{17.5}$ in G22). Above this compositions are fairly constant ($An_{17\pm3}$) in the upper part of the MG and the entire QMG. Olivine compositions vary from $Fo_{40\text{-}4}$ in the profile as a whole with $Fo_{40\text{-}36}$ in TZ, $Fo_{29\text{-}6}$ in MG and $Fo_{5\text{-}4}$ in QMG. Ca-poor pyroxenes have an overall compositional range from $Mg\#opx_{57\text{-}13}$ with $Mg\#opx_{57\text{-}49}$ in MCU IVf, $Mg\#opx_{53\text{-}49}$ in TZ, $Mg\#opx_{44\text{-}15}$ in MG and $Mg\#opx_{17\text{-}13}$ in QMG. Ca-rich pyroxenes vary from $Mg\#cpx_{65\text{-}20}$ with $Mg\#cpx_{65\text{-}59}$ in MCU IVf, $Mg\#cpx_{64\text{-}61}$ in TZ, $Mg\#cpx_{56\text{-}21}$ in MG and $Mg\#cpx_{25\text{-}20}$ in QMG. The plagioclase component of mesoperthite in QMG varies between An_9 and An_{15} whereas the orthoclase component varies between Or_{96} and Or_{97} (Tables 2 and 3).

Compositional variations of the mafic silicates and plagioclase with stratigraphic height take place throughout MCU IVf, TZ and the lower half of the MG-unit where all solid-solution phases in Fig. 4 become more evolved upwards. Above this minerals have essentially constant, low-temperature compositions in the upper MG and throughout the QMG.

Samples from different sub-profiles generally show reasonable compositional agreement, such as where the Drange and Grøning sub-profiles overlap in the lower part of the MG-unit and where the Grøning and Podlå sub-profiles overlap in the lower part of the QMG-unit. The fact that mineral compositions near the base of the QMG-unit are more or less constant in Fig. 4 implies that the precise relative locations of the

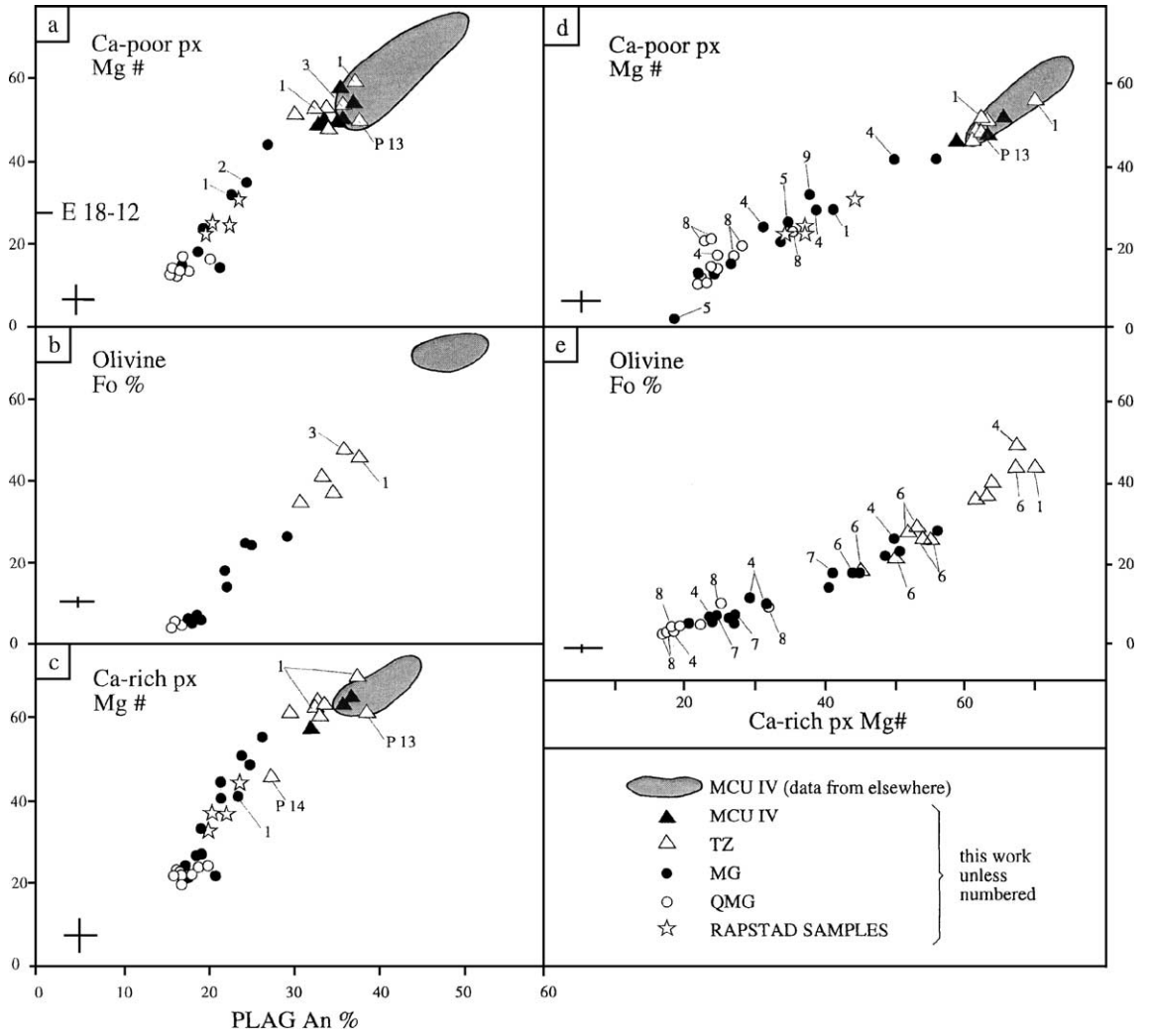

Fig. 5. Compositional covariation of mineral pairs in the upper part of the Bjerkreim-Sokndal layered intrusion. (a) An% in plagioclase vs. Mg# in Ca-poor pyroxene. The MCU IV field contains 106 points (3 outlying points have been omitted). (b) An% in plagioclase vs. Fo% in olivine. The MCU IV (zone b) field contains 54 points (1 outlying point omitted). (c) An% in plagioclase vs. Mg# in Ca-rich pyroxene. The MCU IV (zones e+f) field contains 43 points (2 outlying points omitted). (d) Mg# in Ca-poor pyroxene vs. Mg# in Ca-rich pyroxene. The MCU IV (zones e+f) field contains 42 points (1 outlying point omitted). (e) Fo% in olivine vs. Mg# in Ca-rich pyroxene. Data sources for the numbered points: 1: Schiellerup (1991); 2: Nielsen et al., (1996); 3: Holdam (1990); 4: Duchesne and Wilmart (1997); 5: Nielsen (1992); 6: Duchesne et al. (1987); 7: Duchesne (1972); 8: Rietmeijer (1979); 9: Nielsen (1988). Data sources for MCU IV field: 1, 2, 3 and 9 above plus Kirkegaard (1991) and Jensen et al. (1993). All unnumbered points are from the present work and are listed in Tables 1, 2 and 3. The two anomalous samples P13 and P14 are identified in (c) and P13 in (a); see text for details. Error bars are at the two standard deviation level. Ca-poor pyroxene data in E18-12 is from Nielsen (1992).

lowermost samples in the Podlå sub-profile and the uppermost ones at Grøning are not critical for interpretations. Samples G29-27 and D52-53 from the lower part of the MG-unit generally lie on trends towards more evolved mineral compositions upwards so that their relative locations in Fig. 4 seem reasonable. According to Fig. 3, sample P12 is located in the lower part of the MG unit but its mineral compositions in Fig. 4 (particularly the Ca-rich pyroxene) are more consistent with a location in the upper portion of this unit. For the sake of convenience, P12 is located, with some degree of uncertainty,

Table 1
Selected mineral compositions from the Podlå (P), Grøning (G) and Drange (D) sub-profiles

A. Plagioclase compositions

Sample	P1	P6	G20	G24	G28	D50	D47	D42
Lithology	QMG	QMG	MG	MG	MG	TZ	TZ	MCU IVf
SiO_2%	65.05	65.22	64.52	64.91	63.85	60.24	59.77	59.06
Al_2O_3%	22.23	22.28	22.19	22.51	23.05	24.41	24.74	25.22
FeO%	0.07	0.07	0.11	0.1	0.08	0.08	0.07	0.13
CaO%	3.44	3.48	3.55	3.89	4.46	6.15	6.66	7.25
Na_2O%	9.49	9.42	9.43	9.24	8.94	7.84	7.42	6.79
K_2O%	0.32	0.37	0.62	0.41	0.45	0.8	0.93	0.71
Total	100.6	100.84	100.42	101.06	100.83	99.52	99.59	99.16
Cations on the basis of 8 oxygens								
Si	2.8509	2.8514	2.8408	2.8364	2.8025	2.7015	2.6823	2.6601
Al	1.1481	1.148	1.1516	1.1592	1.1926	1.2901	1.3087	1.3388
Fe	0.0024	0.0025	0.0039	0.0038	0.0031	0.0032	0.0027	0.0047
Ca	0.1617	0.1631	0.1673	0.1821	0.2099	0.2954	0.3201	0.3499
Na	0.8061	0.7985	0.8049	0.7825	0.7608	0.6812	0.6459	0.5929
K	0.0177	0.0208	0.0349	0.0226	0.025	0.0456	0.0531	0.0411
Sum	4.9869	4.9843	5.0034	4.9866	4.9939	5.017	5.0128	4.9875
An%	16.7	17	17.2	18.9	21.6	30.2	33.1	37.1

B. Olivine compositions

Sample	P6	G20	G24	G28	D50	D47
SiO_2%	30.62	30.74	30.86	31.6	33.51	34.31
FeO%	65.76	65.51	65.52	61.19	50.32	47.64
MnO%	1.52	1.38	1.29	1.12	0.61	0.61
MgO%	1.81	2.32	2.59	6.02	15.61	17.97
Total	99.71	99.95	100.26	99.93	100.05	100.53
Cations on the basis of 4 oxygens						
Si	1.0182	1.0171	1.0159	1.0168	1.0085	1.0108
Fe	1.8302	1.8124	1.8037	1.6466	1.2664	1.1736
Mn	0.0428	0.0387	0.0361	0.0306	0.0155	0.0151
Mg	0.0899	0.1147	0.1273	0.2889	0.7005	0.7891
Sum	2.9811	2.9829	2.983	2.9829	2.9909	2.9886
Fo%	4.7	6	6.6	14.9	35.6	40.2

C. Ca-rich pyroxene sub-solidus compositions

Sample	P1	P6	G20	G24	G28	D50	D47	D42
SiO_2%	49.54	49.27	49.59	50.16	50.58	51.66	51.91	52.01
TiO_2%	0.12	0.16	0.09	0.12	0.21	0.28	0.33	0.26
Al_2O_3%	0.64	0.84	0.76	0.73	1.04	1.61	1.76	0.82
FeO%	24.54	25.21	24.57	23.23	19.54	12.87	12.31	11.94
MnO%	0.6	0.62	0.57	0.48	0.49	0.26	0.28	0.29
MgO%	4	3.44	4.34	4.89	7.49	11.5	12.4	12.62
CaO%	19.76	19.6	19.15	20.12	19.84	20.39	20.13	20.87
Na_2O%	0.43	0.5	0.39	0.49	0.5	0.53	0.54	0.49
Total	99.63	99.64	99.46	100.22	99.69	99.1	99.66	99.3

(continued on next page)

Table 1 (*continued*)

C. Ca-rich pyroxene sub-solidus compositions

Sample	P1	P6	G20	G24	G28	D50	D47	D42
Cations on basis of 6 oxygens								
Si	1.995	1.9905	1.9959	1.9936	1.9837	1.9731	1.9643	1.9779
Ti	0.0036	0.0048	0.0027	0.0037	0.0061	0.0079	0.0094	0.0075
Al	0.0305	0.0402	0.0361	0.0341	0.0481	0.0724	0.0784	0.037
Fe	0.8264	0.8519	0.8268	0.7722	0.6409	0.4111	0.3897	0.3797
Mn	0.0205	0.0211	0.0194	0.0161	0.0162	0.0086	0.0089	0.0092
Mg	0.2403	0.2074	0.2605	0.2898	0.4377	0.655	0.6996	0.7155
Ca	0.8525	0.8485	0.8259	0.857	0.8335	0.8346	0.8162	0.8503
Na	0.034	0.0394	0.0308	0.0374	0.0382	0.0396	0.0399	0.0365
Sum	4.0028	4.0038	3.9981	4.0039	4.0044	4.0023	4.0064	4.0136
Mg#cpx	22.5	19.6	24	27.3	40.6	61.4	64.2	65.3

D. Ca-poor pyroxene sub-solidus compositions

Sample	P1	G20	D50	D42
SiO_2	46.63	47.72	51.37	51.82
TiO_2	0.08	0.1	0.13	0.14
Al_2O3	0.21	0.19	0.69	0
FeO	45.92	45.78	29.16	27.73
MnO	1.63	1.23	0.53	0.63
MgO	4.31	4.61	16.88	18.54
CaO	0.88	0.73	0.92	0.74
Total	99.66	100.36	99.68	99.6
Cations on basis of 6 oxygens				
Si	1.9856	2.0035	1.9862	1.9927
Ti	0.0027	0.0032	0.0037	0.004
Al	0.0104	0.0093	0.0314	0
Fe	1.6353	1.6074	0.9429	0.8916
Mn	0.0587	0.0436	0.0172	0.0205
Mg	0.2736	0.2885	0.9731	1.063
Ca	0.0402	0.0327	0.0382	0.0306
Sum	4.0065	3.9882	3.9927	4.0024
Mg#opx	14.3	15.2	50.8	54.4

Lithologies: MCU IVf=Megacyclic Unit IVf; MG=mangerite; QMG=quartz mangerite.
Most of the compositions are the average of 9 analyses (3 points in each of 3 grains).
Exsolution features have been avoided in the pyroxenes.

in the upper part of the MG-unit in Fig. 4; no weight is attached to this sample in the following.

The importance of the new mineral chemical data presented here is illustrated in Fig. 5 where it is plotted together with other published and unpublished data from BKSK. In Fig. 5a, plagioclase and Ca-poor pyroxene compositions from MCU IV lie in a broad, elongate field extending from about An_{52}:Mg#opx_{75} to about An_{36}:Mg#opx_{48}. The most primitive TZ samples overlap with the evolved end of the MCU IV field and the evolved TZ samples extend towards the MG and QMG compositions. The TZ and MG samples together cover a wide compositional range (from about An_{37}:Mg#opx_{58} to about An_{18}:Mg#$_{17}$) whereas the QMG samples have fairly constant, highly evolved compositions, centring around An_{16}:Mg#opx_{15}.

Olivine is restricted to the lower part (zone IVb) of MCU IV and does not re-appear until the TZ. This compositional gap is evident in Fig. 5b where MCU IVb samples lie in a field with compositions in the range $Fo_{75\text{-}67}$ and $An_{53\text{-}44}$ whereas the most primitive compositions in TZ are Fo_{47} and An_{37}, respectively. The TZ, MG and QMG samples constitute a continuous, elongate trend, reaching Fo_4:An_{16} in the most

Table 2
Mineral compositions in the Drange subprofile (and 4 additional samples)

Sample no.	D41	D42	D43	D44	D45	D46	D47	D48	D49
Zone	MCU IV f	MCU IV f	MCU IV f	MCU IV f	MCU IV f	MCU IV f	TZ	TZ	TZ
An%	35.3	37.1	36.2	33.3	35	32.6	33.1	33.7	34
Mg#opx	56.9	54.4	50.2	48.7	50.4	49	a	49.1	52.6
Fo%	a	a	a	a	a	a	40.2	a	37.7
Mg#cpx	a	65.3	62.9	a	a	58.6	64.2	60.7	63.3

Sample no.	D50	D51	D52	D53	G17	G29	P13	P14
Zone	TZ	MG	MG	MG	QMG	MG	TZ?	TZ?
An%	30.2	26.4	24.5	21.5	18.6	25.3	38.6	26.9
Mg#opx	50.8	44.2	a	a	16.9	a	49.7	a
Fo%	35.6	29.2	22.7	18.6	a	22.4	a	a
Mg#cpx	61.4	56.3	50.3	44.8	24.1	48.9	62	46.2
Meso An%					12.2	26.6		
Meso Or%					95.5	87.6		

Whole rock geochemical analyses have not been carried out on the Drange samples or on samples G17, G29, P13 and P14. a=absent.
Meso An%/Or% Composition of the plagioclase/orthoclase component in mesoperthite.

evolved QMG sample. Clinopyroxene is present in the upper part of MCU IV (zones IVe and IVf) and the overlying TZ, MG and QMG; coexisting plagioclases and clinopyroxenes show a continuous evolutionary compositional trend in Fig. 5c. Two pyroxenes coexist in MCU IV throughout zones IVe and IVf and in some of the TZ, MG and QMG samples. The narrow, elongate trend in Fig. 5d implies that the two pyroxenes are in compositional equilibrium. The overall compositional range for pyroxene pairs in Fig. 5d is from Mg#opx:Mg#cpx 69:74 to 6:19. Olivine and clinopyroxene only coexist in the uppermost part of BKSK in some of the TZ, MG and QMG samples; these form a narrow, elongate compositional trend in Fig. 5e. A plot of olivine vs. Ca-poor pyroxene compositions has not been included since these phases only coexist in a few TZ, MG and QMG samples.

The anomalous compositions of samples P13 and P14 mentioned earlier are apparent in Fig. 5a and c. P13 is equivalent to the upper part of zone IVf or the lower part of TZ (but contains no olivine) whereas P14 is equivalent to the lower part of the MG-unit. Both samples come from isolated outcrops, the locations of which (Fig. 3) would predict that P13 should be more evolved than P14. Since the opposite is clearly the case and their compositions are widely different, these samples are ignored in the following.

While considering mineral chemistry it is worth noting that the TZ sample E18-12 (from Fig. 2 and Table 1 in Nielsen et al., 1996) has an anomalous composition. No plagioclase composition was published for this sample. In Fig. 5a it is clear that a Ca-poor pyroxene composition of $Mg\#opx_{28}$ is much more evolved than any of the TZ samples studied here (which lie in the range $Mg\#opx_{49\text{-}53}$). This sample also has an elevated Sr-isotopic ratio (0.71094) that is much higher than any other published value from BKSK (MG and QMG: 0.7085) and approaches values reported from the surrounding gneisses (e.g. 0.7196; Versteeve, 1975). We therefore suggest that this sample is not representative of the TZ and has probably been subjected to contamination by gneissic material. It should certainly be disregarded in petrogenetic discussions of the BKSK.

The four Rapstad samples have plagioclase compositions in the range $An_{24\text{-}20}$, Ca-poor pyroxene $Mg\#opx_{32\text{-}24}$ and Ca-rich pyroxene $Mg\#cpx_{45\text{-}33}$. In Fig. 5 they plot broadly in the middle of the MG field, despite the fact that they all contain quartz and three of them are QMGs. The Rapstad samples therefore have significantly more primitive mineral compositions than the QMGs from the profile in Fig. 4.

3.4. Whole rock geochemistry

Whole-rock chemical analyses have been carried out by X-ray fluorescence (XRF) using a Philips PW 2400 spectrometer at the Department of Earth

Table 3
Whole rock geochemical data and mineral compositions for samples from the Grøning (G) and Podlå (P) sub-profiles and from the Rapstad area

Sample nos.	G28	G27	G26	G24	G23	G22	G21	G20	G19	G18	P12	P11	P9	P8	P7	P6	P5	P4	P2	P1	RAP1	RAP2	RAP3	RAP4
Lithology	MG	MG	MG	MG	MG	MG	MG	MG	MG	QMG	MG	QMG	QMG	QMG	QMG	QMG	QMG	CHARN	QMG	QMG				
SiO_2%	54.4	56.2	56.4	57.5	53.3	54.4	54.6	53.6	56.1	60.6	57.9	59.8	61.2	61.9	63.8	64.4	65.1	77.2	64.2	64.7	55.12	58.72	57.47	60.57
TiO_2	1.76	1.37	1.32	1.23	2.28	1.76	1.76	1.88	1.45	1.03	0.94	1.09	1.02	1	0.86	0.83	0.85	0.17	0.92	0.82	2.18	1.66	1.74	1.46
Al_2O_3	16	16.7	16.6	16.5	14	14.4	14.3	14.1	15.4	15.4	16.1	16.1	15.7	15.9	14.6	14.4	14.5	11.7	14.6	14.6	14.69	14.36	14.57	14.05
Fe_2O_3	3.26	2.7	3.2	2.84	3.75	6.5	1.71	2.21	2.76	2.35	3.04	2.21	2.77	2	2.55	2.04	2.23	0.75	1.81	2.32	2.76	2.14	2.63	3.07
FeO	7.64	6.43	6.02	6.21	10.59	7.19	11.5	12.57	8.95	6.11	6.45	6.13	5.4	5.15	4.34	5.01	4.18	0.51	4.76	4.18	8.29	7.19	7.34	5.94
MnO	0.19	0.16	0.13	0.16	0.24	0.21	0.27	0.27	0.22	0.16	0.18	0.16	0.14	0.12	0.11	0.13	0.13	0.02	0.12	0.11	0.18	0.16	0.18	0.14
MgO	1.37	1.09	1.02	0.75	1.19	0.79	1.28	1.05	0.9	0.54	0.56	0.79	0.48	0.52	0.4	0.34	0.42	0.1	0.45	0.41	2.11	1.39	1.46	1.03
CaO	4.59	4.06	3.95	3.44	4.51	4.64	4.54	4.59	4.06	2.9	3.55	3.25	2.54	2.39	2.22	2.15	1.78	0.52	1.87	2.13	4.58	3.79	3.87	3.25
Na_2O	4.67	4.87	4.78	5.07	4.2	4.45	4.41	4.29	4.45	4.51	4.87	4.71	4.4	4.44	4.1	3.96	3.99	3.18	4.21	4.06	4.54	4.07	4.54	4.32
K_2O	4.1	4.51	4.67	4.73	4.12	3.88	3.85	3.93	4.29	5.15	4.69	4.47	5.61	5.7	5.53	5.51	5.69	4.9	5.72	5.48	3.73	4.44	4.14	4.5
P_2O_5	0.76	0.66	0.64	0.52	0.64	0.51	0.68	0.57	0.58	0.27	0.3	0.33	0.24	0.24	0.19	0.18	0.19	0.01	0.19	0.17	0.85	0.65	0.68	0.48
BaO	0.395	0.441	0.428	0.298	0.223	0.147	0.24	0.227	0.297	0.181	0.163	0.151	0.158	0.18	0.112	0.111	0.143	0.06	0.109	0.118	0.11	0.117	0.111	0.106
H_2O	0.82	0.66	0.8	0.65	0.74	1.13	0.7	0.72	0.66	0.65	1.2	0.81	0.43	0.41	0.54	0.51	0.44	0.37	0.51	0.43	0.59	0.61	0.68	0.66
Total	99.96	99.85	99.96	99.9	99.78	100.01	99.84	100.01	100.12	99.85	99.94	100	100.09	99.95	99.35	99.57	99.64	99.49	99.47	99.53	99.7	99.3	99.4	99.58
V ppm	35	28	19	21	31	36	35	33	22	18	20	24	16	17	14	13	14	<	14	14	78	38	40	34
Cr	<	<	5	<	<	<	<	<	<	<	5	9	<	<	9	<	13	<	12	11	<	<	<	<
Ni	3	2	3	2	2	3	3	3	4	2	4	5	3	<	2	<	3	<	<	<	9	8	8	7
Cu	12	9	12	9	12	15	20	20	18	10	12	18	11	13	10	10	14	<	9	12	19	15	18	16
Zn	132	112	103	114	176	139	210	213	160	154	176	173	134	155	122	118	154	30	137	103	190	151	203	162
Ce	42	36	45	49	60	75	88	77	84	80	72	102	95	86	86	93	93	34	103	88	129	129	135	121
Rb	44	51	56	69	52	45	48	56	59	87	67	77	109	102	118	124	136	108	124	119	57	84	77	81
Sr	344	363	352	226	190	152	233	227	240	184	202	225	133	158	101	100	166	40	96	102	289	233	234	191
Y	27	25	29	27	36	39	56	50	57	54	52	68	65	63	50	59	64	6	56	58	70	69	74	64
Zr	66	83	126	119	182	77	96	69	104	299	136	790	451	140	557	665	601	153	612	658	744	753	766	814
Nb	4	4	5	5	11	9	21	7	17	23	12	19	26	13	27	29	19	4	28	22	28	30	31	20
Pb	8	8	9	10	9	8	11	11	15	16	15	19	20	22	20	19	24	19	21	18	17	21	18	19
Mg€	15	14	14	11	10	10	10	8	9	8	8	11	8	9	8	6	9	16	9	9	20	16	17	15
Plag. An%	21.6	n.a.	19.3	18.9	n.a.	17.5	18.6	17.2	20.8	16.4	17.8	19.9	17.8	n.a.	15.8	17	16.4	12.7	15.9	16.7	24.1	20.9	23.2	19.8
Mg#opx	a	n.a.	23.4	a	n.a.	a	18.4	15.2	15.2	a	a	16.7	14	n.a.	12.9	a	13.9	a	14.6	14.3	32	26.1	25.2	24
Fo%	14.9	n.a.	a	6.6	n.a.	a	6.9	6	a	5.2	5.1	a	a	n.a.	4.4	4.7	a	a	a	a	a	a	a	a
Mg#cpx	40.6	n.a.	34.1	27.3	n.a.	21.2	27	24	21.1	22.5	21	24.6	21.7	n.a.	a	19.6	21.1	n.a.	21.6	22.5	44.8	37.1	37.2	32.8
Meso-An%	17	n.a.	14.5	12	n.a.	12.9	16.9	14.6	17.5	8.8	12.8	15.4	12.4	n.a.	12.3	11.4	12.4	11.3	8.3	10.9	a	a	a	a
Meso Or%	88.3	n.a.	92.4	94.7	n.a.	95.6	93.1	94.1	94.3	96.1	95.2	95.9	95.9	n.a.	96.5	96.8	97.1	97.4	96.9	96.4	a	a	a	a

<=below detection limit.
n.a.=not analysed.
a=mineral absent.
Mg€ =100 MgO/(MgO+FeO).
Mg#=100 Mg/(Mg+Fetot).

Sciences, University of Aarhus. Major elements were analysed on glass tablets whereas traces were analysed on pressed powders. FeO was determined by potassium dichromate titration. Results are presented in Table 3. Detection limits (in ppm) for trace elements that are present in low concentrations are V=5, Cr=4, Ni=2, Cu=1.

Selected major elements for the 20 Grøning and Podlå samples in Table 3 (10 MGs, 9 QMGs and one charnockite) show well-constrained trends with decreasing MgO, P_2O_5 and TiO_2 with increasing SiO_2 (Fig. 6a–c). There is a clear break in slope from the MG- to the QMG-samples, and the charnockite lies on a distant extension of the QMG trend. In Fig. 6d, K_2O generally increases with increasing SiO_2 in the MGs whereas most of the QMGs have fairly constant K_2O values (ca. 5.6% K_2O) with SiO_2 ranging from 61–66%. The charnockite sample, with 77.2% SiO_2 and 4.90% K_2O, lies far to the right of the QMGs.

The concentration of Sr varies between 152 and 363 ppm in the MGs and has generally lower values

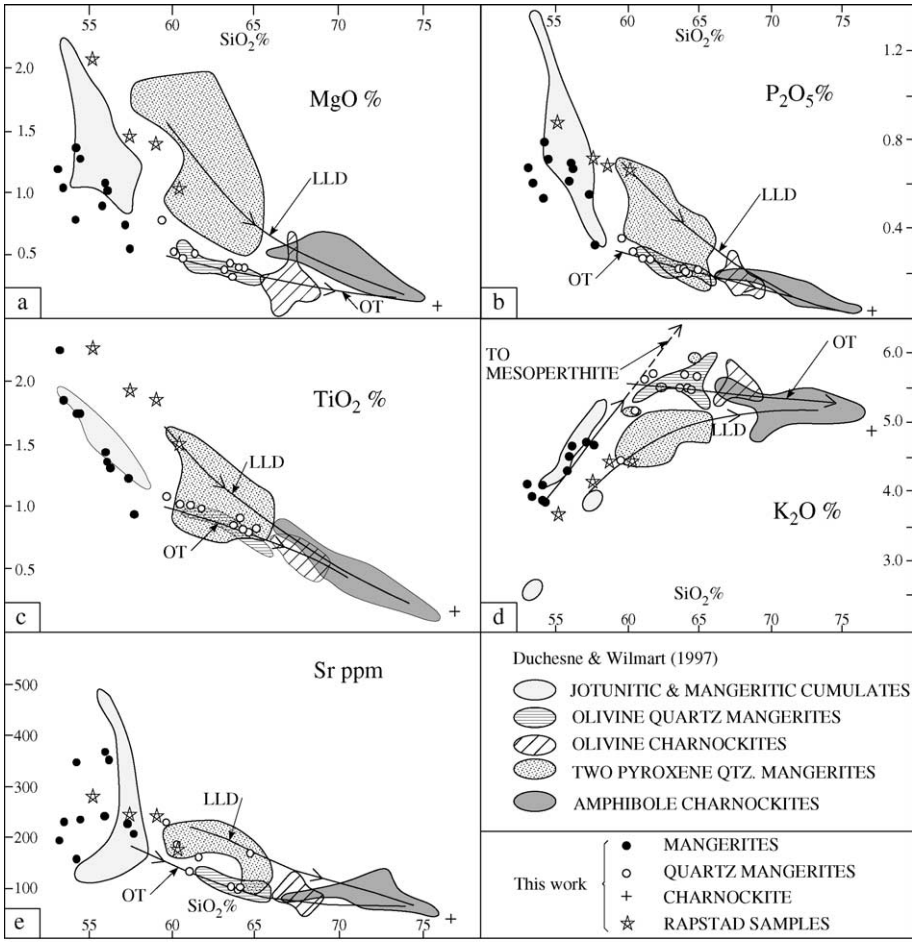

Fig. 6. Whole rock geochemical compositional variation in the upper part of the Bjerkreim-Sokndal layered intrusion. Evolutionary trends from Duchesne and Wilmart (1997) (D&W): LLD=main jotunitic liquid line of descent; OT=olivine trend. Diagram shows SiO_2 % vs. (a) MgO%, (b) P_2O_5%, (c) TiO_2%, (d) K_2O% and (e) Sr ppm. Mangerites from this study are compositionally similar to the jotunitic and mangeritic cumulate field of D&W, whereas our quartz mangerites lie close to their olivine QMG field. The four Rapstad samples form an extension of D&W's LLD-trend to more primitive compositions.

(225–96 ppm) in the QMGs (Fig. 6e). Other trace elements are present in concentrations typical for these evolved rocks. There are, for example, very low values of Cr (<13 ppm) and Ni (<5 ppm), fairly low concentrations of V which enters Fe–Ti oxides (<36 ppm) and low to moderate values of Cu (<20 ppm), Zn (<213 ppm) and Pb (<24 ppm) which preferably enter sulphides. Zirconium is present in concentrations up to 299 ppm in zircon-free samples and between 451 and 790 ppm in zircon-bearing QMGs. Barium, which enters the feldspar structure, is present in concentrations between ca. 0.15% and 0.44% BaO in the MGs and 0.11–0.18% BaO in the QMGs. Rubidium ranges from 44–69 ppm in the MGs, increasing to 77–136 ppm in the QMGs.

We have chosen diagrams of TiO_2, MgO, K_2O, P_2O_5 and Sr vs. SiO_2 to illustrate the compositional variation of our whole-rock analyses in Fig. 6 because these are key plots in Duchesne and Wilmart (1997) who identified two distinct geochemical trends in the evolved rocks of BKSK. One, which they called the main liquid line of descent (LLD in Fig. 6), comprises two-pyroxene QMGs and extends to amphibole charnockites. The second trend, defined by their olivine-bearing QMGs and charnockites, is referred to as the olivine-bearing trend (OT in Fig. 6).

Our MG samples plot close to or within the jotunitic and MG field of Duchesne and Wilmart (1997). In Fig. 6d the elongate MG field points towards the composition of mesoperthite and Duchesne and Wilmart (1997) considered that this is essentially a cumulate trend in which the compositional variation is largely controlled by the modal amount of alkali feldspar (mesoperthite; Fig. 6d). Our QMG samples plot in or very close to the field of olivine QMGs and our charnockite sample has a composition very close to the most evolved amphibole charnockite in Fig. 6.

The four Rapstad QMG samples (Table 3) have compositions that are clearly different from our Podlå and Grøning MGs and QMGs in most of the plots in Fig. 6. For corresponding SiO_2 contents they have significantly more MgO and TiO_2 and contain more P_2O_5 and less K_2O. One of the Rapstad samples lies consistently in the two-pyroxene QMG field of Duchesne and Wilmart whereas the other three form an extension of this field to more primitive compositions.

4. Discussion

4.1. Magma influx in the upper part of the Bjerkreim-Sokndal layered intrusion

BKSK is characterised by compositional regressions at the bases of the megacyclic units that developed in response to major events of magma addition to the chamber (Fig. 2). There are no compositional regressions with stratigraphic height in Fig. 4 that spans the interval from zone IVf to the QMGs. In the only previous study across this interval, Duchesne and Wilmart (1997) found a regression in the vicinity of the MG/QMG boundary located in an enclave-rich zone in the Ørsland area (Fig. 1b). In terms of mineral compositions this was defined by a regression in Mg#cpx from ca. 22 (which would be in equilibrium with plagioclase $An_{18\pm2}$; Fig. 5) at the top of the MG unit to a maximum of $Mg\#cpx_{35}$ in the enclave-rich zone (in equilibrium with $An_{22\pm2}$). The latter composition is equivalent to that some 350 m lower in the MG-unit (Fig. 8 in Duchesne and Wilmart, 1997). This reversal is minor compared with, for example, that at the MCU III-IV boundary where the cumulate assemblage changes from apatite–bearing gabbronorite (with plagioclase of An_{45}) to troctolite (with An_{55}). Since there is no evidence of a compositional reversal at the MG/QMG boundary (or elsewhere) in Fig. 4 there could not have been any major, chamber-wide influx of new, relatively primitive, dense magma into the BKSK intrusion at this time. We therefore consider that the reversal in the Ørsland area represents either a minor, local magma influx or local contamination as a result of country rock assimilation, an alternative that was also suggested by Duchesne and Wilmart (1997, p. 353).

4.2. Cumulate status of the rocks

There is no doubt that the rocks belonging to the BKSK Layered Series are cumulates, even though primary igneous textures are generally masked as a result of extensive recrystallisation. Apart from the presence of modal layering, the sequence from MCU IVf through the TZ to the middle of the MG-unit (Fig. 4) shows clear evidence of fractional crystallisation. The successive upward appearance of antiperthitic plagioclase, Fe-rich olivine and abundant mesoper-

thite is accompanied by increasingly evolved mineral compositions. The cumulate status of the uppermost MGs and QMG-unit and charnockites is, however, not so obvious. Modal layering is generally absent and mineral compositions are essentially constant in these highly evolved rocks (Fig. 4). The generally massive nature of the rocks and extensive recrystallisation mean that cumulus textures, even if they were originally present, are not identifiable. These rocks have extremely evolved compositions and clearly crystallised from liquids close to the granite minimum in the Q-Ab-Or phase diagram. However, the fact that the amount of normative quartz (which is a good proxy for modal quartz in these rocks) increases systematically upwards in the QMGs, accompanied by a systematic increase in normative Or, implies that the rocks are cumulates. This is supported by the appearance of zircon in the QMG. The fact that the amount of normative quartz increases upwards through most of the QMG (Fig. 4) probably reflects a gradual, upward increase in the amount of intercumulus quartz in the quartz mangeritic cumulates.

We suggest that the gradually increasing amounts of normative quartz and orthoclase in the MGs and QMGs imply that they crystallised from liquids that were evolving towards the granitic (charnockitic) minimum in the residua system. If it is accepted that they are cumulates, the transition from MG to QMG simply reflects the appearance of intercumulus quartz. In the field the boundary between these units has been defined by the presence of macroscopic quartz; this is when there is approximately 5% modal quartz. While this is a very useful field criterion, the appearance of an intercumulus phase is not a significant petrological boundary and simply reflects increasing amounts of trapped, evolved liquid. The QMGs can strictly be considered as a unit transitional between the underlying mangeritic cumulates and the overlying charnockites that essentially represent liquid compositions. The only new cumulus phase to appear in the QMG-unit is zircon.

An interesting feature in Fig. 4 is that *Q* and *Or* both increase as far as the charnockite sample, after which they decrease (Fig. 4). According to Fig. 9 in Bolle et al. (2000), the top of sub-profile P is close to the axial zone of the syncline. This raises the intriguing possibility that the charnockite sample (P4) comes from the synclinal core and that the QMG samples P1 and P2 come from the northern limb of the syncline. An alternative possibility is that the charnockite represents the crystalline products of a lens of charnockitic liquid that became trapped in the vicinity of the roof of the intrusion. Future work will shed more light on these issues.

The MG-unit was suggested by Duchesne et al. (1987) to be a sequence of flotation cumulates formed by the accumulation of buoyant mesoperthite at the roof of the magma chamber. They envisaged that the roof was located at the level now occupied by the xenolith-rich interval and that the QMGs form a separate intrusion, as was previously suggested by Wiebe (1984). We agree that the MGs are cumulates but consider that the QMGs form a continuation of the Layered Series bottom cumulates, as suggested by Duchesne and Wilmart (1997).

The role of feldspars in the MG- and QMG-units is open to debate. Cumulus plagioclase becomes antiperthitic near the top of MCU IVf and in relatively undeformed rocks there is evidence that it was joined by interstitial alkali feldspar in the TZ. At the base of MG the cumulus feldspar becomes mesoperthitic and there only appears to have been one original feldspar phase which has subsequently exsolved to mesoperthite. The presence in our MG and QMG samples of plagioclase as a minor phase adjacent to K-rich feldspar could therefore be a result of the extensive recrystallisation of mesoperthite. It thus appears likely that only one cumulus feldspar crystallised throughout most of the the evolution of BKSK.

4.3. Two immiscible silicate liquids?

A noteworthy feature in Fig. 2 is that whereas the compositions of Ca-rich pyroxene and plagioclase gradually become more evolved through MCU IV, they become rapidly more evolved through the Transition Zone and the lower part of the mangerite unit. The fact that the rate as which the mineral compositions become evolved increases towards the top of MCU IV could imply that the volume of magma remaining in the chamber was significantly decreasing. There is, however, a thickness of more than ca. 1500 m of more evolved rocks above the top of MCU IV (Fig. 4). Another feature is that the Transition Zone is considerably more mafic than the overlying mangerite (e.g. Duchesne et al., 1987). Both

these features are difficult to explain in terms of the progressive fractionation of a single magma. A possible explanation involves liquid immiscibility; this has been suggested by Wiebe (1979) to have played a role during the late stages of crystallisation of the Nain anorthosite complex in Labrador.

Experimental work by Philpotts (1981) demonstrated that liquid immiscibility developed in melts of mixtures between jotunite and quartz mangerite. One melt was relatively Si-poor and Fe-rich; the conjugate melt was Si- and alkali-rich. In the light of this work it seems possible that liquid immiscibility could have developed in BKSK.

A possible scenario is that the initial jotunitic parental magma to BKSK at some stage started to separate out a Si- and alkali-rich immiscible liquid which was buoyant and rose to the top of the chamber. The volume of this buoyant magma layer gradually increased as immiscibility progressed during fractional crystallisation of the main volume of underlying magma. The two immiscible liquids would remain in chemical and thermal equilibrium so that they could crystallise minerals of the same composition but in different amounts. Here we envisage that relatively mafic underlying magma crystallised to completion at the top of the Transition Zone and that the TZ-mangerite boundary marks the onset of crystallisation of the overlying, immiscible, felsic magma. Other simultaneous processes, such as magma replenishment and assimilation of country rocks, would no doubt disturb the system to some extent. However, there is sufficient evidence to suggest the possible role of liquid immiscibility during evolution of the BKSK. Nevertheless, in melting experiments performed by Vander Auwera et al. (1998) on jotunites of appropriate compositions for BKSK parental magmas, no evidence of immiscibility was observed. This topic clearly requires further investigation.

4.4. The OT and LLD trends and the Rapstad samples

This paper is mainly concerned with stratigraphic compositional variations from the upper part of the Layered Series to the highly evolved overlying lithologies as developed in the composite profile in Fig. 4. This sequence is interpreted as representing the crystalline products of fractional crystallisation of the magma remaining in the chamber after development of the underlying cumulates. This is consistent with the rocks belonging to the "olivine trend" of Duchesne and Wilmart (1997). Our MG samples lie in or very close to the olivine-bearing jotunite/MG field of Duchesne and Wilmart (1997). The compositional variation of these cumulates is largely controlled by the role of cumulus mesoperthite (Fig. 6), combined with the increasingly iron-rich compositions of the mafic phases upwards (Fig. 4). The olivine QMG to olivine charnockite trend is, to a large extent, one of increasing SiO_2-content and is interpreted as reflecting the increasing role of intercumulus quartz while the composition of the mafic phases remains essentially constant. Detailed petrographic study has revealed the presence of small relict (often corroded) olivine grains in most of our QMG samples. It is therefore possible that olivine was originally present in most, if not all, of the "olivine trend" samples but that it has subsequently disappeared as a result of subsolidus reactions.

Our stratigraphic profile does not contain any samples that belong to the two-pyroxene QMG trend. However, the four Rapstad samples from the broadly quartz mangeritic unit that is discordant to the jotunitic TZ and its overlying mangerite (Fig. 1) have petrographic features that are similar to those described for the two-pyroxene QMG by Duchesne and Wilmart (1997). The mineral chemistry of the Rapstad samples is also distinctive (Fig. 5) with relatively primitive mineral compositions. The chemical compositions of these samples (Fig. 6) are consistent with their representing an extension of the two-pyroxene QMG trend of Duchesne and Wilmart (1997) to slightly more primitive compositions.

It therefore seems likely that the Rapstad samples belong to a discordant unit of quartz mangerite that was intruded into the uppermost part of BKSK. Many intrusive bodies of this affinity were emplaced into the BKSK roof zone where they crystallised to form two-pyroxene QMG and amphibole charnockites (Duchesne and Wilmart, 1997). In the field it is very difficult to distinguish between lithologies belonging to the olivine trend that represent a continuation of the Layered Series and two-pyroxene-bearing lithologies that are intrusive into the former. One useful feature for future studies will probably prove to be the xenolith-rich zone near the MG-QMG boundary that should be truncated by any younger intrusions.

4.5. Inclusions in the upper part of BKSK and the source of the "LLD" magma

The upper part of the Layered Series locally contains numerous xenoliths of mostly quartzo-feldspathic to noritic gneisses that represent fragments of country rocks. Modal layering below some inclusions is depressed or disrupted whereas that above drapes over xenoliths. Some outcrops contain numerous, tabular xenoliths with thicknesses up to a few centimeters that can be traced for several meters along strike. These tabular bodies are conformable with modal layering and have no obvious influence on its orientation. When the BKSK layered intrusion is "unfolded" it has the form of a broad saucer (Nielsen et al., 1996). A consequence of this is that the interface between the magma at the top of the chamber and the country rocks belonging to the roof comprised a very large surface area. The roof of BKSK is not preserved but it seems unlikely that there was extensive crystallisation down from the roof. Magma chambers with small aspect ratios emplaced into relatively cold rocks at high levels in the crust may crystallise inwards from the walls and down from the roof, as well as upwards from the floor, as is the case for the Skærgaard Intrusion (Wager and Brown, 1968). Layered intrusions with large aspect ratios emplaced into relatively hot rocks at deep crustal levels are commonly subject to repeated magma influxes and most of the crystallisation is up from the floor, as is the case for the Stillwater (McCallum, 1996) and Bushveld (Eales and Cawthorn, 1996) Intrusions. The Fongen-Hyllingen layered intrusion that was emplaced at a higher crustal level than BKSK shows no evidence of crystallisation down from the roof (Wilson and Sørensen, 1996). The source of country rock inclusions in BKSK is therefore essentially restricted to feeder channel(s) or the roof. Some inclusions may have been transported into the BKSK chamber during successive magma influxes, but the main source seems likely to have been the roof.

If their densities were high enough, fragments falling off the roof would sink through the magma and impact on the floor. It seems likely that the magma in the BKSK chamber was compositionally zoned with evolved, buoyant, cooler magma at the roof and more primitive, denser, hotter magma at the floor (Nielsen and Wilson, 1991). If they did not have a high enough density to reach the floor, country rock xenoliths would sink to their level of neutral buoyancy and then remain suspended in the magma until they became enveloped by the advancing floor cumulates. During this prolonged period of suspension in the compositionally zoned magma they would be able to equilibrate with the enveloping melt. Since the country rock gneisses had considerably higher Sr-isotopic ratios than the BKSK parental magma (Nielsen et al., 1996), this would be an efficient mechanism for the development of isotopic contamination of the resident magma. This process may have been partly responsible for the correlation between mineral compositions and Sr-isotopic signatures in the upper part of the Layered Series. This feature is otherwise difficult to explain in BKSK since fractional crystallisation (which essentially controls mineral compositions) takes place at the floor, whereas assimilation (which controls isotopic signatures) would normally take place at the roof.

This explanation may be valid for at least some of the gneissic inclusions in the upper part of BKSK but it does not explain the locally large concentration of inclusions near the MG/QMG boundary, the "septum xenolithique" of Michot (1960). The lithologies of the inclusions at this interval are highly variable (inhomogeneous quartzo-feldspathic gneisses, norites, amphibolites, leucogranites) and it is inconceivable that they all had the same density. The most likely explanation for the concentration of country rock inclusions with different lithologies, and therefore variable densities, at this stratigraphic level is that they became dislodged from the roof when this level was the floor of the chamber i.e. the crystallisation front when quartz had become a consistent intercumulus phase, comprising approximately 5% of the rock.

A study of inclusions in the Skærgaard Intrusion (Irvine et al., 1998) has revealed that the roof collapsed repeatedly during crystallisation of the Layered Series. These collapse events cannot have been triggered by magma replenishment episodes since there is no evidence for more than one influx of magma into the Skærgaard chamber. In chambers subjected to repeated replenishment it does, however, seem likely that periodic roof collapse may be triggered by expansion of the chamber as a result of magma influx. Turbulence in the uppermost part of a

magma chamber as a result of large scale convective overturn could also be responsible for disruption of the roof. As discussed above there is no compositional reversal in the Bjerkreim lobe in the vicinity of the MG/QMG boundary that could indicate that a replenishment event took place at this time (Fig. 4). However, Duchesne and Wilmart (1997) presented convincing evidence for the existence of the crystallisation products of two compositionally distinct quartz mangeritic to charnockitic magmas in the uppermost part of the BKSK chamber. These belong to the olivine trend (OT, comagmatic with the Layered Series) and the main liquid line of descent (LLD, related to a separate jotunitic melt).

Accepting that the QMGs and charnockites belonging to the "olivine trend" (OT) are a product of continued fractional crystallisation after formation of the Layered Series there are two possible sources for the origin of the two-pyroxene QMG and amphibole charnockites (LLD trend). An internal source for the LLD-magma would involve an isolated buoyant roof melt and its convective overturn with the resident OT-magma at the time represented by the xenolith-rich interval near the MG-QMG boundary. In the light of the discovery reported here of an intrusive body of QMG of LLD-affinity at Rapstad, an external source seems, however, more likely.

An external source for the LLD-magma was suggested by Duchesne and Wilmart (1997). Evidence for the availability of compositionally appropriate melts at about the right time is provided by the magmas emplaced into the so-called Apophysis (Bolle, 1996; Duchesne and Wilmart, 1997). It seems established that mingling of two magmas (one parental to QMG; one producing jotunitic pillows) did take place at the time represented by the MG-QMG boundary (Wiebe, 1984). This intrusive event may have been much more voluminous and complex than previously recognised. The addition of low-density melts to the chamber could have increased the density contrast at the roof, sufficient to initiate major collapse.

5. Conclusions

(a) The upper part of the Bjerkreim lobe of the Bjerkreim-Sokndal layered intrusion consists of two suites of evolved rocks. One is genetically related to the underlying Layered Series and comprises olivine-bearing jotunites, mangerites, quartz mangerites and charnockites. The other suite consists of jotunites, mangerites, quartz mangerites and charnockites that contain two pyroxenes and no olivine. These observations are in accordance with those of Duchesne and Wilmart (1997) who demonstrated that the two suites are geochemically distinct.

(b) Mineral compositions in a stratigraphic profile through the olivine-bearing suite in the upper part of the Bjerkreim lobe become increasingly evolved through MCU IVf and the jotunitic Transition Zone into the middle section of the mangerite unit. Above this mafic minerals have fairly constant, low-temperature compositions that persist into the quartz mangerite unit.

(c) This olivine-bearing TZ-MG-QMG sequence represents a series of increasingly evolved cumulates with the successive appearance of iron-rich olivine, followed by mesoperthite and zircon. Quartz becomes an increasingly voluminous intercumulus phase above the upper part of the mangerite unit. The normative orthoclase content of the rocks also increases upwards, reflecting changes in the composition of the cumulus feldspar.

(d) The absence of compositional regressions in mineral chemistry in this stratigraphic sequence implies that there was no chamber-wide influx of primitive magma during crystallisation of the upper part of the cumulate sequence.

(e) It is possible that two immiscible silicate liquids could have developed during evolution of BKSK.

(f) A laterally persistent xenolith-rich unit near the MG-QMG boundary represents a major episode of roof collapse during the final stages of crystallisation of BKSK.

(g) Quartz mangerites in the Rapsatd area are discordant to the MCU IV-TZ-MG sequence. Samples from the Rapstad intrusive body have compositional affinities with the two-pyroxene quartz mangerites of Duchesne and Wilmart (1997). The Rapstad body supports their suggestion that the BKSK was intruded by evolved melt(s) during or after the final stages of crystallisation of the resident magma.

Acknowledgements

The first author is indebted to Jean-Clair Duchesne for introduction to Bjerkreim-Sokndal in 1984 and for subsequent scientific cooperation. We are also very grateful to Brian Robins for helping us to understand the workings of the Bjerkreim-Sokndal magma chamber. Financial support to study BKSK was provided by Danish Natural Science Research Council grants. We would like to thank Sidsel Grundvig for help with the microprobe and XRF analyses. The manuscript was improved as a result of reviews by Bob Wiebe and Olivier Bolle.

References

Bolle, O., 1996. L'Apophyse du Massif Stratiforme de Bjerkreim-Sokndal (Rogaland, Norvege): Une Intrusion Composite de la Suite Charnockitique. In: Demaiffe, D. (Ed.), Petrology and Geochemistry of Magmatic Suites of Rocks in the Continental and Oceanic Crusts. A volume dedicated to Professor Jean Michot. Université Libre de Bruxelles, pp. 129–144.

Bolle, O., Diot, H., Duchesne, J.C., 2000. Magnetic fabrics and deformation in charnockitic igneous rocks of the Bjerkreim-Sokndal layered intrusion (Rogaland, Southwest Norway). Journal of Structural Geology 22, 647–667.

Demaiffe, D., Duchesne, J.C., Hertogen, J., 1979. Trace element variations and isotopic compositions of charnockitic acidic rocks related to anorthosites (Rogaland, S.W. Norway). In: Ahrens, L.H. (Ed.), Origin and Distribution of the Elements. Pergamon Press, Oxford, pp. 417–429.

Demaiffe, D., Weis, D., Michot, J., Duchesne, J.C., 1986. Isotopic constraints on the genesis of the anorthositic suite of rocks. Chemical Geology 57, 167–179.

Duchesne, J.C., 1972. Fe–Ti oxide minerals in the Bjerkreim-Sokndal massif (Norway). Journal of Petrology 13, 57–81.

Duchesne, J.C., 1987. The Bjerkreim-Sokndal massif. In: Maijer, C., Padget, P. (Eds.), The Geology of Southernmost Norway. Norges geologiske undersøkelse Special Publications, vol. 1, pp. 56–59.

Duchesne, J.C., Demaiffe, D., 1978. Trace elements and anorthosite genesis. Earth and Planetary Science Letters 38, 249–272.

Duchesne, J.C., Wilmart, E., 1997. Igneous charnockites and related rocks from the Bjerkreim-Sokndal Layered Intrusion (Southwest Norway): a jotunitie (hypersthene monzodiorite)-derived A-type granitoid suite. Journal of Petrology 38, 337–369.

Duchesne, J.C., Denoiseux, B., Hertogen, J., 1987. The norite-mangerite relationships in the Bjerkreim-Sokndal layered lopolith (SW Norway). Lithos 20, 1–17.

Eales, H.V., Cawthorn, R.G., 1996. The Bushveld Complex. In: Cawthorn, R.G. (Ed.), Layered Intrusions. Elsevier, Amsterdam, pp. 2181–2230.

Glazner, A.F., 1994. Foundering of mafic plutons and density stratification of continental crust. Geology 22, 435–438.

Holdam, H.K., 1990. Bjerkreim-Sokndal Intrusionen, Sydnorge: En undersøgelse af den nordlige flankes petrologi og mineralkemi. Unpublished M.Sc. thesis. Department of Earth Sciences, University of Aarhus.

Irvine, T.N., 1982. Terminology for Layered Intrusions. Journal of Petrology 23, 127–162.

Irvine, T.N., Andersen, J.C.Ø., Brooks, C.K., 1998. Included blocks (and blocks within blocks) in the Skaergaard intrusion. Geological relations and the origins of rhythmic modally graded layers. Geological Society of America Bulletin 110 (11), 1398–1447.

Jensen, J.C., Nielsen, F.M., Duchesne, J.C., Demaiffe, D., Wilson, J.R., 1993. Magma influx and mixing in the Bjerkreim-Sokndal layered intrusion, South Norway: evidence from the boundary between two macrocyclic units at Storeknuten. Lithos 29, 311–325.

Kirkegaard, J.B., 1991. Petrologien i den sydvestlige flanke af Bjerkreim-Sokndal Intrusionen, SV Norge. Unpublished M.Sc. thesis. Department of Earth Sciences, University of Aarhus.

McCallum, I.S., 1996. The Stillwater Complex. In: Cawthorn, R.G. (Ed.), Layered Intrusions. Elsevier, Amsterdam, pp. 441–484.

Michot, P., 1960. La géologie de la catazone: le problème des anorthosites, la palingenèse basique et la tectonique catazonale dans le Rogaland méridonale (Norvège méridionale). Norges Geologiske Undersøkelse 212, 1–54.

Michot, J., 1961. The anorthositic complex of Haaland-Helleren. Norsk Geologisk Tidsskrift 41, 157–172.

Michot, P., 1965. Le magma plagioclasique. Geologische Rundschau 54, 956–976.

Michot, J., Pasteels, P., 1969. La variation du rapport/87Sr/86Sr)0 dans les roches génétiquement associées au magma plagioclasique (Premiers resultants). Annales de la Société Géologique de Belgique 92, 255–262.

Nielsen, F.M., 1988. En petrologisk og mineralkemisk undersøgelse af den Lagdelte Serie I Bjerkreim-Sokndal Intrusionen, Sydnorge. Unpublished M.Sc. thesis, Department of Earth Sciences, University of Aarhus.

Nielsen, F.M., 1992. Magmakammerprocesser belyst med udgangspunkt i Bjerkreim-Sokndal intrusionen, Rogaland, Sydnorge. Unpublished Ph.D. thesis, Department of Earth Sciences, University of Aarhus.

Nielsen, F.M., Wilson, J.R., 1991. Crystallisation processes in the Bjerkreim-Sokndal layered intrusion, South Norway: evidence from the boundary between two macrocyclic units. Contributions to Mineralogy and Petrology 107, 403–414.

Nielsen, F.M., Campbell, I.H., McCulloch, M., Wilson, J.R., 1996. A strontium isotopic investigation of the Bjerkreim-Sokndal layered intrusion, Southwest Norway. Journal of Petrology 37, 171–193.

Overgaard, G., 1998. Forholdet mellem den lagdelte serie og de overliggende udviklede bjergarter i Bjerkreim-Sokndal intrusionen, Sydnorge. Unpublished M.Sc. thesis, Department of Earth Sciences, University of Aarhus.

Paludan, J., Hansen, U.B., Olesen, N.Ø., 1994. Structural evolution of the Precambrian Bjerkreim-Sokndal intrusion, South Norway. Norsk Geologisk Tidsskrift 74, 185–198.

Pasteels, P., Michot, J., Lavreau, J., 1970. Le complexe éruptiv du Rogaland méridional (Norvège). Signification pétrogénétique de la farsundite et de la mangérite quartzique des unités orientales: arguments géochronologiques et isotopiques. Annales de la Société Géologique de Belgique 93, 453–476.

Philpotts, A.R., 1981. A model for the generation of massif-type anorthosites. Canadian Mineralogist 19, 233–253.

Rietmeijer, F.J.M., 1979. Pyroxenes from iron-rich igneous rocks in Rogaland, SW Norway. Geologica Ultrajectina 21 (341pp.)

Schärer, U., Wilmart, E., Duchesne, J.C., 1996. The short duration and anorogenic character of anorthositic magmatism: U–Pb dating of the Rogaland complex, Norway. Earth and Planetary Science Letters 139, 335–350.

Schiellerup, H., 1991. Bjerkreim-Sokndal Intrusionen. En petrologisk, mineral-og geokemisk undersøgelse af Bjerkreimloben i området omkring Helleland. Unpublished M.Sc. thesis, Department of Earth Sciences, University of Aarhus.

Vander Auwera, J., Longhi, J., Duchesne, J.C., 1998. A liquid line of descent of the jotunite (hypersthene monzodiorite) suite. Journal of Petrology 39, 439–468.

Versteeve, A.J., 1975. Isotope geochronology in the high-grade metamorphic Precambrian of southwestern Norway. Norges geologiske undersøkelse 318, 1–50.

Wager, L.R., Brown, G.M., 1968. Layered Igneous Rocks. Oliver and Boyd, Edinburgh. 588 pp.

Wiebe, R.A., 1979. Fractionation and liquid immiscibility in an Anorthositic Pluton of the Nain Complex, Labrador. Journal of Petrology 20, 239–269.

Wiebe, R.A., 1984. Commingling of magmas in the Bjerkreim-Sogndal lopolith (Southwest Norway): evidence for the compositions of residual liquids. Lithos 17, 171–188.

Wielens, J.B.W., Andriessen, P.A.M., Boelrijk, N.A.I.M., Hebeda, E.H., Priem, H.N.A., Verdurmen, E.A.T., Verschure, R.H., 1980. Isotope geochronology in the high-grade metamorphic Precambrian of southwestern Norway: New data and interpretations. Norges Geologiske Undersøkelse 359, 1–30.

Wilson, J.R., Sørensen, H.S., 1996. The fongen-hyllingen layered intrusive complex. In: Cawthorn, R.G. (Ed.), Layered Intrusions. Elsevier, Amsterdam, pp. 303–330.

Wilson, J.R., Robins, B., Nielsen, F.M., Duchesne, J.C., Vander Auwera, J., 1996. The Bjerkreim-Sokndal layered intrusion, Southwest Norway. In: Cawthorn, R.G. (Ed.), Layered Intrusions. Elsevier, Amsterdam, pp. 231–255.